Journal of Alloys and Compounds 509 (2011) 2929–2932

Contents lists available at ScienceDirect

Journal of Alloys and Compounds

journal homepage: www.elsevier.com/locate/jallcom

Electromagnetic wave absorption properties of mechanically mixed $Nd_2Fe_{14}B/C$ microparticles

Xianguo Liu [a,b], Siu Wing Or [b,*], S.L. Ho [b], Dianyu Geng [a], Zhigao Xie [a], Han Wang [a], Zhidong Zhang [a]

[a] Shenyang National Laboratory for Materials Science, Institute of Metal Research and International Centre for Materials Physics, Chinese Academy of Sciences, Shenyang 110016, PR China

[b] Department of Electrical Engineering, The Hong Kong Polytechnic University, Hung Hom, Kowloon, Hong Kong

ARTICLE INFO

Article history:
Received 20 September 2010
Received in revised form
22 November 2010
Accepted 22 November 2010
Available online 30 November 2010

Keywords:
Carbon
Complex permeability
Complex permittivity
Electromagnetic wave absorption
$Nd_2Fe_{14}B$
Reflection loss

ABSTRACT

$Nd_2Fe_{14}B/C$ microparticles were prepared by a mechanical mixing technique using a weight ratio of 2:1. Paraffin-bonded $Nd_2Fe_{14}B/C$ composites were fabricated using 40 wt% microparticles, and their electromagnetic wave absorption properties were studied and compared with those of the paraffin-bonded $Nd_2Fe_{14}B$ composites in the 2–18 GHz frequency range and for 1–5 mm thickness. The $Nd_2Fe_{14}B/C$–paraffin composites exhibit dual dielectric resonance in complex relative permittivity (ε_r) and essentially flat response in complex relative permeability (μ_r) rather than showing an abrupt change in both ε_r and μ_r as in the $Nd_2Fe_{14}B$–paraffin composites. The results are ascribed to the increased electrical resistivity in the $Nd_2Fe_{14}B/C$-paraffin composites and the protection on the magnetic properties of the $Nd_2Fe_{14}B$ microparticles at 2–18 GHz by the presence of the C phase. Large reflection loss (RL) exceeding −10 dB and an optimal RL of −13.2 dB are achieved in the $Nd_2Fe_{14}B/C$–paraffin composites from 9.6 to 18 GHz at a thickness of 1.4–2.6 mm and at 18 GHz at a thickness of 1.4 mm, respectively.

1. Introduction

The rapid development and expanding use of electrical and electronic devices and systems such as personal mobile phones, local area networks, radar systems, satellite systems, power systems, renewable energy systems, and transportation systems have greatly increased the impact of electromagnetic interference (EMI) on humans and the environment [1–5]. In fact, there is a great demand for electromagnetic (EM) wave absorbers operating in the microwave (or GHz) frequency range in order to tackle the problems associated with EMI pollution. In principle, a good EM wave absorber should effectively absorb EM waves at frequencies of interest and with a low density, a thin thickness, and a low production cost. Ferrites and ferromagnetic metals are regarded as traditional EM wave absorption materials for high frequencies. Ferrites generally possess a high magnetic permeability and a low power loss at the expense of exhibiting a negative temperature coefficient of resistivity and a small saturation magnetization. By contrast, ferromagnetic metals have a large saturation magnetization and a high Snoek limit, but their magnetic permeability decreases, power loss increases, and temperature increases with the increase in operational frequency due to the presence of high eddy-current losses caused by a low electrical resistivity. For this reason, ferromagnetic metals in the particulate form of sizes smaller than the skin depth (e.g., 1 μm for Fe in the 1–5 GHz range) are utilized to minimize the effects of eddy currents [6–9]. Nevertheless, the density of ferromagnetic metals is considered to be too high for use in fast developing smart electronics.

In the recent decade, some nanostructured granular composites of magnetic and dielectric nanoparticles have been reported, including α-Fe/SmO, α-Fe/Y_2O_3, Fe/Fe_3B/Y_2O_3, etc. However, the finite interface makes the two different nanoparticles difficult to establish a good matching between the dielectric and magnetic properties, resulting in low EM wave absorption properties in general [10–12]. Alternatively, C-coated nanocapsules with magnetic nanoparticles as the core and C as the shell have been formed to provide improved EM matching and property tailorability via the combination of dielectric and magnetic materials in a single nanocapsule. Typical examples include C-coated Fe, Ni, Co, FeNi, FeCo, and FeNiMo nanocapsules [13–17]. Unfortunately, the complex preparation process, low repeatability, and poor machining properties impede their application viability.

$Nd_2Fe_{14}B$ sintered microparticles have been widely used in electromagnetic devices and electrical machines owing to their excellent magnetic properties and mature preparation process [18]. The drawback of significant eddy-current losses induced at microwave frequencies makes them hardly to be used as a good EM wave absorber. By combining the magnetic advantageous of

* Corresponding author. Tel.: +852 34003345; fax: +852 23301544.
E-mail address: eeswor@polyu.edu.hk (S.W. Or).

0925-8388/$ – see front matter © 2010 Elsevier B.V. All rights reserved.
doi:10.1016/j.jallcom.2010.11.161

$Nd_2Fe_{14}B$ with the light-weight, high absorbability, and good EM matchability of C, it can realize a relatively high-performance and cost-effective EM wave absorption material. In this paper, we prepare mechanically mixed $Nd_2Fe_{14}B$/C microparticles and disperse them in a paraffin matrix to form paraffin-bonded $Nd_2Fe_{14}B$/C composites in order to investigate the frequency and thickness dependences on their EM wave absorption properties. A special attention is put on the influence of C on the resulting EM wave absorption properties of the as-prepared microparticles in comparison with the $Nd_2Fe_{14}B$ microparticles.

2. Experimental details

$Nd_2Fe_{14}B$ microparticles and C powders were commercially acquired with an average particle/powder size of 5 μm. 5 g of $Nd_2Fe_{14}B$ microparticles and C powders was weighted using a weight ratio of 2:1 and sealed in a hardened steel vial with steel balls of 12 mm diameter under normal atmosphere. Mechanical mixing was performed in a low-speed ball-milling machine with a rotational speed of 40 rpm for 30 min, resulting in $Nd_2Fe_{14}B$/C microparticles. The morphology of the as-prepared $Nd_2Fe_{14}B$/C microparticles was examined using a scanning electron microscope (SEM) (Philips SSX-550) with an emission voltage of 20 kV.

To enable the study of the EM wave absorption properties of both $Nd_2Fe_{14}B$/C and $Nd_2Fe_{14}B$ microparticles, paraffin-bonded $Nd_2Fe_{14}B$/C composites (or $Nd_2Fe_{14}B$/C–paraffin composites) and paraffin-bonded $Nd_2Fe_{14}B$ composites (or $Nd_2Fe_{14}B$–paraffin composites), both in the shape of toroid of dimensions 7 mm outer diameter and 3 mm inner diameter, were prepared by uniformly dispersing 40 wt% $Nd_2Fe_{14}B$/C microparticles and 40 wt% $Nd_2Fe_{14}B$ microparticles in a paraffin matrix, respectively. It is known that paraffin is an electrical insulator and a non-magnetic material so that it is transparent to EM waves. The EM wave absorption properties of both types of composites were evaluated by measuring their complex relative permittivity ($\varepsilon_r = \varepsilon'_r - j\varepsilon''_r$, where ε'_r and ε''_r are the real and imaginary parts of ε_r, respectively) and complex relative permeability ($\mu_r = \mu'_r - j\mu''_r$, where μ'_r and μ'' are the real and imaginary parts of μ_r, respectively) from 2 to 18 GHz using a network analyzer (Agilent 8722ES). The frequency (f) dependence of reflection loss (RL) was calculated from the measured ε_r and μ_r at a given composite thickness (d) using the following expressions: [3–5,10–14]

$$Z_{in} = Z_0 \left(\frac{\mu_r}{\varepsilon_r}\right)^{1/2} \tanh\left[j\left(\frac{2\pi f d}{c}\right)(\mu_r \varepsilon_r)^{1/2}\right] \quad (1)$$

$$\mathrm{RL} = 20\log\left|\frac{Z_{in} - Z_0}{Z_{in} + Z_0}\right| \quad (2)$$

where Z_{in} is the input impedance of absorber, Z_0 is the characteristic impedance of air, and $c = 3 \times 10^8$ m/s is the velocity of light.

3. Results and discussion

Fig. 1 shows the SEM image and energy dispersive spectrum (EDS) of the as-prepared $Nd_2Fe_{14}B$/C microparticles. From Fig. 1(a), it is clear that the microparticles have irregular shapes and their longest dimension varies from 1 to 10 μm with an average value of 3.4 μm. This average value is smaller than the average particle size of 5 μm of the $Nd_2Fe_{14}B$ microparticles because of the comminuting effect during ball milling. The microparticles can be treated as isotropic due to the good mixing of the $Nd_2Fe_{14}B$ microparticles and the C powders. As shown in Fig. 1(b), C, Nd, and Fe elements are detected by EDS, but B element is not found. This is because light elements such as H and B are difficult to be detected by EDS.

Fig. 2(a) and (b) shows the frequency (f) dependence of complex relative permittivity ($\varepsilon_r = \varepsilon'_r - j\varepsilon''_r$) of the $Nd_2Fe_{14}B$–paraffin composites and the $Nd_2Fe_{14}B$/C–paraffin composites at a thickness (d) of 2 mm, respectively. It is noted that the real (ε'_r) and imaginary (ε''_r) parts of ε_r indicate the polarization and dielectric loss of the composites, respectively. It is seen that the two types of composites exhibit quite different ε_r characteristics in the 2–18 GHz range. The $Nd_2Fe_{14}B$–paraffin composites in Fig. 2(a) show a strong peak in ε''_r at 6.8 GHz, together with a rapid drop in ε'_r from 5 to 9 GHz, suggesting a dielectric resonance at 6.8 GHz. This dielectric resonance is as expected because the $Nd_2Fe_{14}B$ microparticles are highly conductive and the skin effect becomes very significant at microwave frequencies [19,20]. For the $Nd_2Fe_{14}B$/C–paraffin composites in Fig. 2(b), dual dielectric resonance is detected at 10.8 and 14.8 GHz.

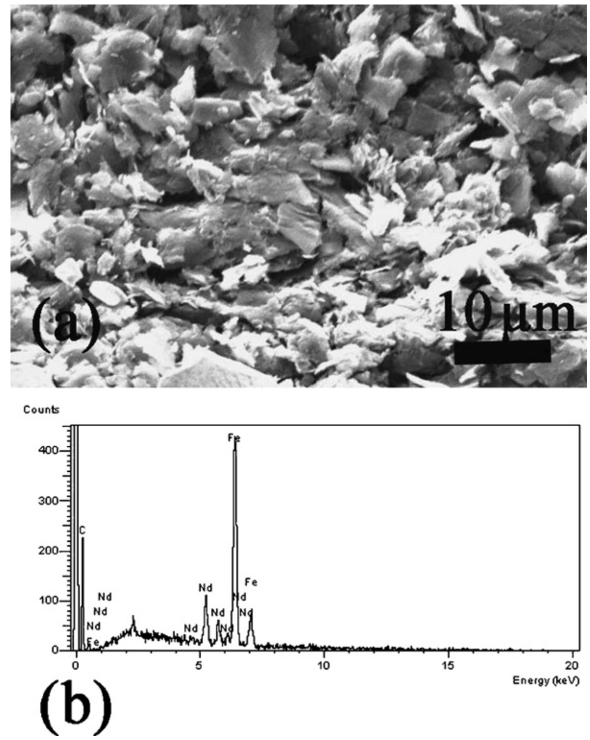

Fig. 1. (a) SEM image and (b) EDS of as-prepared $Nd_2Fe_{14}B$/C microparticles.

This dual dielectric resonance is mainly caused by a redistribution process of charges periodically occurred between the $Nd_2Fe_{14}B$ and C phases during activation of an EM wave [14]. The presence of such dual dielectric resonance in the $Nd_2Fe_{14}B$/C–paraffin composites indicates that it is a good candidate for EM wave absorbers [14]. In addition, the values of ε'_r (9–10) and ε''_r (0.7–1.36) for the $Nd_2Fe_{14}B$/C–paraffin composites are lower than those (ε'_r = 20–180 and ε''_r = 48–148) for the $Nd_2Fe_{14}B$–paraffin composites due to the increased electrical resistivity by the contribution of the C phase to the $Nd_2Fe_{14}B$/C–paraffin composites, according to the free electron theory [4].

Bovda et al. reported that the electrical resistivity of $Nd_2Fe_{14}B$ is $\sim 1.6 \times 10^{-6}$ Ω m, being close to that of ferromagnetic metals of 10^{-6}–10^{-8} Ω m [21]. In ferromagnetic metal-based composites, the space charge polarization mechanism could be used to explain the

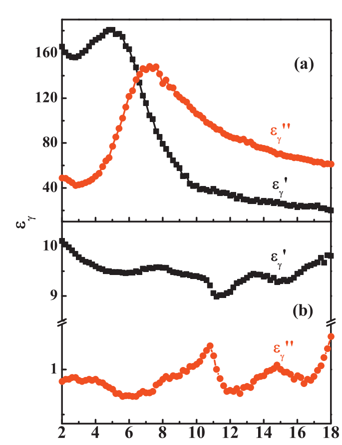

Fig. 2. Frequency (f) dependence of complex relative permittivity ($\varepsilon_r = \varepsilon'_r - j\varepsilon''_r$) of (a) $Nd_2Fe_{14}B$–paraffin composites and (b) $Nd_2Fe_{14}B$/C–paraffin composites at a thickness (d) of 2 mm.

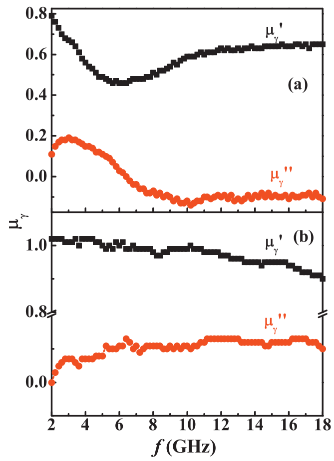

Fig. 3. Frequency dependence (f) of complex relative permeability ($\mu_r = \mu_r' - j\mu_r''$) of (a) $Nd_2Fe_{14}B$–paraffin composites and (b) $Nd_2Fe_{14}B$/C–paraffin composites at a thickness (d) of 2 mm.

frequency dependence of dielectric permittivity since the space charge polarization occurs between adjacent metallic components and contributes to a high dielectric permittivity [22,23]. For the $Nd_2Fe_{14}B$–paraffin composites, the space charge polarization takes place at the interfaces of $Nd_2Fe_{14}B$ microparticles and paraffin matrix in such way that free electrons from the $Nd_2Fe_{14}B$ microparticles promote the charge accumulation at the interfaces and give a high dielectric permittivity. It is consistent with the case of ferromagnetic metal-based composites in which the metallic components serve as the source of abundant electrons [22,23]. In the $Nd_2Fe_{14}B$/C–paraffin composites, the space charge polarization is weakened due to the existence of the C phase, which prevents the $Nd_2Fe_{14}B$ phase from forming electrical conducting networks so that the electrical resistivity of the $Nd_2Fe_{14}B$/C–paraffin composites is increased [15].

Fig. 3(a) and (b) shows the frequency dependence (f) of complex relative permeability ($\mu_r = \mu_r' - j\mu_r''$) of the $Nd_2Fe_{14}B$–paraffin composites and the $Nd_2Fe_{14}B$/C–paraffin composites at a thickness (d) of 2 mm, respectively. For the $Nd_2Fe_{14}B$–paraffin composites in Fig. 3(a), the real (μ_r') and imaginary (μ_r'') parts of μ_r exhibit a magnetic resonance at 3 GHz. In fact, μ_r' decreases initially from 0.79 to 0.46 in the 2–6 GHz range; it then increases from 0.46 to 0.61 in the 6–11 GHz range and remains almost constant at 0.61 above 11 GHz. If we compare the obtained μ_r' (<0.79 in general) with the nanocapsules (1.0–1.1 for C-coated FeNi nanocapsules), the reduced μ_r' in the $Nd_2Fe_{14}B$–paraffin composites is mainly due to the influence of eddy-currents on the $Nd_2Fe_{14}B$ microparticles. On the other hand, μ_r'' peaks at 3 GHz with a positive value of 0.19; it then decreases with increasing f and its value becomes negative in the 6.6–18 GHz range with a negative peak of −0.14 at 10.2 GHz. Since the magnetic behavior of EM wave absorption materials may be modulated by the dielectric behavior of the materials to achieve EM coupling [24,25], and according to the Maxwell equations, an ac magnetic field can be induced by an ac electric field and be radiated out [24], the negative μ_r'' value in Fig. 3(a) denotes that the magnetic energy is radiated out from the $Nd_2Fe_{14}B$ microparticles and transferred to the electric energy. For the $Nd_2Fe_{14}B$/C–paraffin composites in Fig. 3(b), μ_r' decreases steadily from 1.02 to 0.9 with increasing f, while μ_r'' increases from 0.01 to 0.13 in the 2–6.4 GHz range and keeps almost constant at 0.13 in the 6.4–18 GHz range. This phenomenon not only indicates that the magnetic resonance has a shift to high frequency, but also suggests that the C phase can protect μ_r of the $Nd_2Fe_{14}B$ microparticles in the GHz range. It is beneficial to enhancing EM wave absorption properties from 2 to 18 GHz.

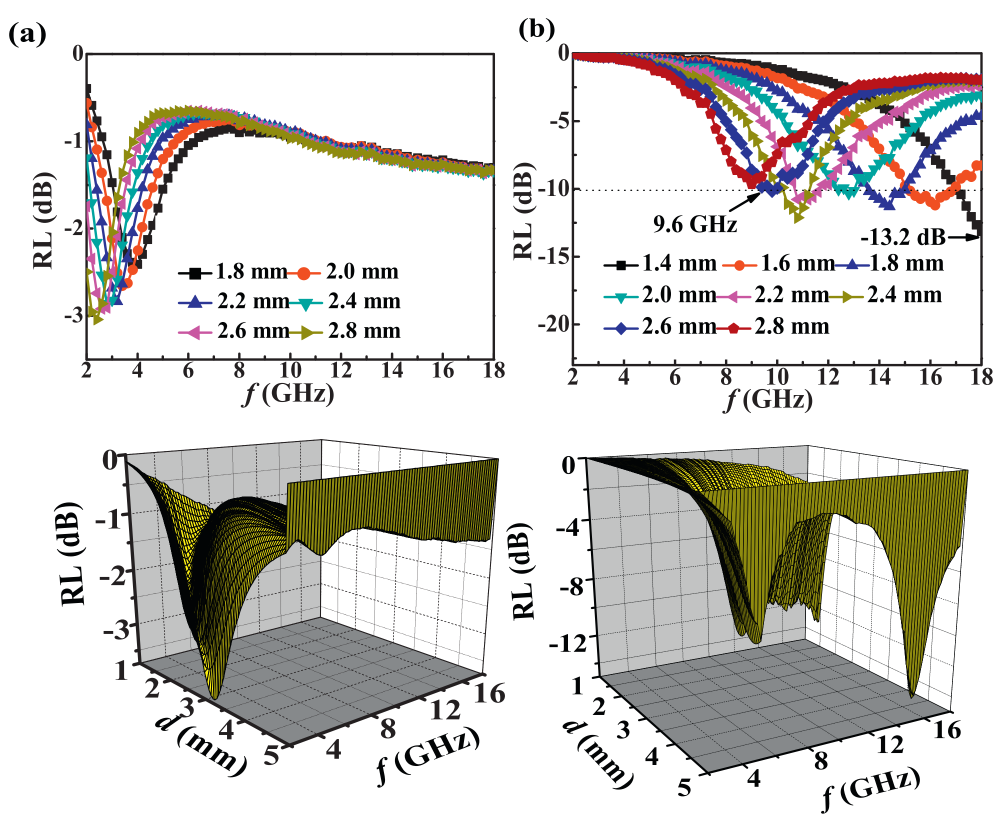

Fig. 4. Reflection loss (RL) as functions of frequency (f) and thickness (d) and three-dimensional maps of RL, f, and d for (a) $Nd_2Fe_{14}B$–paraffin composites and (b) $Nd_2Fe_{14}B$/C–paraffin composites.

Fig. 4(a) and (b) shows the reflection loss (RL) as functions of frequency (*f*) and thickness (*d*) and three-dimensional maps of RL, *f*, and *d* for the $Nd_2Fe_{14}B$–paraffin composites and the $Nd_2Fe_{14}B/C$–paraffin composites, respectively. It is recalled that an absorber with RL exceeding −10 dB, corresponding to 90% attenuation, is generally considered as a good absorber. It is observed that the RL values do not exceed −5 dB in the 2–18 GHz range for all *d* in the $Nd_2Fe_{14}B$–paraffin composites but exceed −10 dB in the 9.6–18 GHz range for *d* = 1.4–2.6 mm in the $Nd_2Fe_{14}B/C$–paraffin composites. In particular, an optimal RL of −13.2 dB is found at 18 GHz for *d* = 1.4 mm in the $Nd_2Fe_{14}B/C$–paraffin composites. This *d* value is smaller than most of nanocomposites of 1.7–2.2 mm [3–17,26,27]. Compared with $Nd_2Fe_{14}B$–paraffin composites, the better EM wave absorption ability exhibited by the $Nd_2Fe_{14}B/C$–paraffin composites can be ascribed to the increased dielectric loss from the enhancement of the electrical resistivity by the C phase, which prevents the $Nd_2Fe_{14}B$ phase from forming electrical conducting networks, and also the enhanced magnetic loss from the protection on μ_r of the $Nd_2Fe_{14}B$ phase by the C phase in the 2–18 GHz range, which makes the magnetic resonance shift to high frequency. Thus, the $Nd_2Fe_{14}B/C$–paraffin composites are a promising candidate for EM wave absorption applications.

4. Conclusion

We have prepared mechanically mixed $Nd_2Fe_{14}B/C$ microparticles and dispersed them in a paraffin matrix to form $Nd_2Fe_{14}B/C$–paraffin composites. The EM wave absorption properties of the composites have been studied as a function of both frequency and thickness, and the results have been compared to those of $Nd_2Fe_{14}B$–paraffin composites. It has been found that the C phase not only can effectively increase the electrical resistivity of the $Nd_2Fe_{14}B/C$–paraffin composites, resulting in dual dielectric resonance in ε_r, but also can protect the magnetic properties of the $Nd_2Fe_{14}B$ microparticles at 2–18 GHz, leading to a shift in the magnetic resonance of the $Nd_2Fe_{14}B$ microparticles shift to high frequency. The enhanced dielectric and magnetic losses from the dual dielectric resonance and magnetic resonance result in good EM absorption properties. Large RL in excess of −10 dB is observed in the $Nd_2Fe_{14}B/C$–paraffin composites from 9.6 to 18 GHz for thickness varying from 1.4 to 2.6 mm, with the optimal RL of −13.2 dB at 18 GHz for 1.4 mm thickness. Therefore, the $Nd_2Fe_{14}B/C$–paraffin composites offer a relatively high-performance and cost-effective solution to absorb EM waves.

Acknowledgments

This work was supported by the National Basic Research Program (2010CB934603) of China, Ministry of Science and Technology of China, the National Natural Science Foundation of China (50831006 and 50701045), and The Hong Kong Polytechnic University Postdoctoral Fellowships Scheme (G-YX3V).

References

[1] A.N. Yusoff, M.H. Abdullah, S.H. Ahmad, S.F. Jusoh, A.A. Mansor, S.A.A. Hamid, J. Appl. Phys. 92 (2002) 876–882.
[2] S.B. Cho, D.H. Kang, J.H. Oh, J. Mater. Sci. 31 (1996) 4719–4722.
[3] X.F. Zhang, X.L. Dong, H. Huang, Y.Y. Liu, W.N. Wang, X.G. Zhu, B. Lv, J.P. Lei, C.G. Lee, Appl. Phys. Lett. 89 (2006) 053115.
[4] X.F. Zhang, X.L. Dong, H. Huang, Y.Y. Liu, B. Lv, J.P. Lei, C.J. Choi, J. Phys. D: Appl. Phys. 40 (2007) 5383–5387.
[5] X.G. Liu, D.Y. Geng, H. Meng, P.J. Shang, Z.D. Zhang, Appl. Phys. Lett. 92 (2008) 173117.
[6] S. Yoshida, J. Magn. Soc. Jpn. 22 (1998) 1353 (in Japanese).
[7] S. Yoshida, M. Sato, E. Sugawara, Y. Shimada, J. Appl. Phys. 85 (1999) 4636.
[8] A. Saito, M. Ogawa, K. Tutui, H. Endo, S. Yahagi, Mater. Jpn. 38 (1999) 46 (in Japanese).
[9] J.L. Snoek, Physica 14 (1948) 207.
[10] S. Sugimoto, T. Maeda, D. Book, T. Kagotani, K. Inomata, M. Homma, H. Ota, Y. Houjou, R. Sato, J. Alloys Compd. 330–332 (2002) 301.
[11] J.R. Liu, M. Itoh, K.I. Machida, Appl. Phys. Lett. 83 (2003) 4017.
[12] J.R. Liu, M. Itoh, K.I. Machida, Chem. Lett. 32 (2003) 394.
[13] X.G. Liu, D.Y. Geng, Z.D. Zhang, Appl. Phys. Lett. 92 (2008) 243110.
[14] X.G. Liu, J.J. Jiang, D.Y. Geng, Z. Han, W. Liu, Z.D. Zhang, Appl. Phys. Lett. 94 (2009) 053119.
[15] X.G. Liu, B. Li, D.Y. Geng, F. Yang, Z.D. Zhang, Carbon 47 (2009) 470–474.
[16] Z. Han, D. Li, H. Wang, X.G. Liu, J. Li, D.Y. Geng, Z.D. Zhang, Appl. Phys. Lett. 95 (2009) 023114.
[17] X.G. Liu, Z.Q. Ou, D.Y. Geng, Z. Han, H. Wang, B. Li, E. Brück, Z.D. Zhang, J. Alloys Compd. 506 (2010) 826–830.
[18] K. Miura, M. Masuda, M. Itoh, T. Horikawa, K. Machida, J. Alloys Compd. 408–412 (2006) 1391–1395.
[19] A.N. Lagarkov, A.K. Saruchev, Phys. Rev. B 53 (1996) 6318.
[20] Y.D. Deng, X. Liu, B. Shen, L. Liu, W.B. Hu, J. Magn. Magn. Mater. 303 (2006) 181–184.
[21] A.M. Bovda, V.A. Bovda, W. Derevyanko, J. Iron Steel Res. Int. 13 (2006) 92–96.
[22] B. Lu, X.L. Dong, H. Huang, X.F. Zhang, X.G. Zhu, J.P. Lei, J.P. Sun, J. Magn. Magn. Mater. 320 (2008) 1106–1111.
[23] S.S. Kim, S.T. Kim, J.M. Ahn, K.H. Kim, J. Magn. Magn. Mater. 271 (2004) 39–45.
[24] X.L. Shi, M.S. Cao, J. Yuan, X.Y. Fang, Appl. Phys. Lett. 95 (2009) 163108.
[25] L. Zhen, J.T. Jiang, W.Z. Shao, C.Y. Xu, Appl. Phys. Lett. 90 (2007) 142907.
[26] X.G. Liu, D.Y. Geng, P.J. Shang, H. Meng, F. Yang, B. Li, D.J. Kang, Z.D. Zhang, J. Phys. D: Appl. Phys. 41 (2008) 175006.
[27] X.G. Liu, D.Y. Geng, H. Meng, W.B. Cui, F. Yang, D.J. Kang, Z.D. Zhang, Solid State Commun. 149 (2009) 47–64.